Energy transfers by long-lived species in glows and afterglows*

S. De Benedictis[‡] and G. Dilecce

Centro di Studio per la Chimica dei Plasmi CNR, Via Orabona 4, 70126 Bari, Italy

Abstract: An overview of the current literature on diagnostics and modeling of energy transfers by long-lived species in N_2–CO, He–NO, He–N_2–O_2, N_2–O_2, and N_2–H_2O plasma is given. Energy transfers by vibrationally excited ground-state long-lived species and by electronic molecular and atomic metastables will be highlighted.

INTRODUCTION

The energy transfers of the various active species present in the plasma, electrons, ions, and neutrals are basic for plasma reactivity. Energy transfers mark the internal state distribution of such species since most of them are state-dependent. In low-temperature plasmas, the distributions are generally nonequilibrium ones [1]. Their shape results from the couplings between the different elementary kinetics involving electrons, ions, atoms, and molecules with different internal excitation. The features of the individual processes can be recognized in the time evolution of the distributions through their characteristic relaxation times [1,2].

The dynamics of energy transfers is mainly studied with species state-selected by laser pump-probe techniques in cell or in atomic-molecular beam under single collision condition. This allows a selective and detailed basis for atomic and molecular dynamic analysis [3–6]. The state of the art of "*State resolved collision induced electronic transitions*" and "*Quenching reactions of electronically excited atoms*" has been reported in two recent reviews by Dagdigian [7] and Setser [8], respectively. Here, we consider energy transfers occurring in glow discharges and afterglows. Addressing energy transfers in a plasma environment is generally less straightforward because of the simultaneous presence of many active species. On the other hand, the large number of excited species makes the plasma a rich source of precursors whose energy transfers must be known for plasma applications. Thus, we address those aspects of energy transfers that are useful for diagnostic purposes as well as for kinetic modeling of glow discharges and afterglows. This is made reviewing the experiments and analysis of energy transfers operated by *long-lived species,* i.e., atoms and molecules in electronic states having a long radiative lifetime (*metastable species*) or atoms in ground electronic state formed in nonequilibrium plasmas. The detection and energy characterization of long-lived species as well as the modeling of their elementary kinetics in various discharge mixtures is an issue of current interest [9], despite the wide literature at disposal (see refs. [1] and [2]). Here we highlight the investigations on collision-induced electronic transitions (CIET) by vibrationally excited molecules (V–E) in CO and NO. CIET by He(2^3S) and N_2($A^3\Sigma_u^+$) metastables in N_2–CO, He–NO, He–N_2–O_2, N_2–O_2, and N_2–H_2O glow and afterglow will be reviewed [10–16].

---

*Lecture presented at the 15th International Symposium on Plasma Chemistry, Orléans, France, 9–13 July 2001. Other presentations are presented in this issue, pp. 317–492.
[‡]Corresponding author

LONG-LIVED SPECIES AND THEIR DETECTION

Low-pressure plasmas in diatomic molecular gases mixtures containing H_2, N_2, O_2, CO, NO, and noble gases are rich of long-lived species like vibrationally excited molecules in the electronic ground state, as well as of atoms and molecules in metastable electronic excited states [17,18].

The highly non-Boltzmann vibrational excitation of the ground electronic state of CO, NO, and N_2 is well known [1,2]. Vibrational populations up to levels v = 40 for CO and v = 23 for NO with extended Treanor plateaus have been detected by infrared emission spectroscopy in both glow discharge [19,20] and in optically pumped cell-system [21]. On the contrary, the plateau in the N_2 vibrational distribution has never been completely detected. Measurements by CARS [22] in a glow discharge detected up to 15 vibrational levels, indicating the existence of a plateau. Recently, a high density (about 0.4 %) of level v = 18 has been measured by cavity ring down spectroscopy (CRDS) in a glow discharge [23]. A high H_2 nonequilibrium degree (v = 0–13), has been measured in [24] by VUV laser spectroscopy, improving the results obtained by CARS and REMPI.

Low-lying electronic states $Ar(^3P)$, $Xe(^3P)$, $Ne(^3P)$, $He(2^1S, 2^3S)$ are metastable and LIF spectroscopy [13] and infrared diode laser absorption [25,26] are used for their detection. Energy transfers in molecular gases have been largely investigated in the afterglow [27,28]. Actually, Xe and Ne metastables are studied as relevant species in the kinetics of microdischarges for plasma-addressed liquid crystal and plasma display panel technologies [29,30].

The $N(^2D, \,^2P)$, $N_2(A^3\Sigma_u^+, a'^1\Sigma_u^-)$, and $O_2(^1\Delta_g)$ metastables, whose relevance in the physical chemistry of the upper atmosphere is well known, are much studied in the laboratory by air-like plasmas [2]. $N_2(A^3\Sigma_u^+, v)$, $N(^4S)$, and $O(^3P)$ take part in reactions leading to the formation of nitric oxide compounds [31]. $N_2(A^3\Sigma_u^+, v)$ has been studied in many environments, and time- and space-resolved investigations have been carried out in electrical discharges [14,32]. Recently, the $N_2(A^3\Sigma_u^+, v = 0)$ space profile in N_2 pink afterglow has been measured by intracavity laser absorption spectroscopy (ICLAS) [33]. Actually, absolute densities of long-lived $N(^4S)$ and $O(^3P)$ are measured by calibrated two-photon absorption laser-induced fluorescence (TALIF) [34,35].

ENERGY TRANSFERS IN POST-DISCHARGES

Post-discharges are useful for studying energy transfers by long-lived species, in particular the quenching of metastables by a target gas, once the environment is properly characterized [17]. In spatial post-discharges, i.e., flowing afterglows, the energy carriers produced in the discharge region flow to the afterglow space region under a null external electric field condition, while in time post-discharges the excitation voltage is switched off almost instantaneously. Post-discharge kinetics is dominated by long-lived species through energy transfers, recombination processes in the gas phase, and diffusion to the walls. In many cases, collision processes are reactive and excited products can also be formed.

The late afterglow is substantially free from energetic electrons, while in the early afterglow the details of the relaxation of the electron energy distribution function (EEDF) are still a matter of study [16,36]. Recently, it has been stressed by modeling of a N_2 microwave afterglow that the EEDF relaxation in post-discharge, due to the presence of a space charge field, is much slower than that obtained assuming a free diffusion regime for electrons [36]. This fact does not affect the fast relaxation of the tail of the EEDF but sustains a high density of low-energy electrons up to few ms in the post-discharge. Furthermore, electron super-elastic collisions with metastables also heat electrons, slowing the relaxation of the electron mean energy [13,36], and forming structures on the EEDF [11]. These effects are also important in supersonic high enthalpy flows [37]. It is, however, difficult to reach a high density of long-lived species in laboratory plasmas. Experimental evidences of electron superelastic structures on EEDF are poor [38]. Indirect evidences have been obtained from the relaxation of excited electronic states of N_2 in post-discharges [12,16]. In Fig. 1 it is reported as an example the time-relaxation of
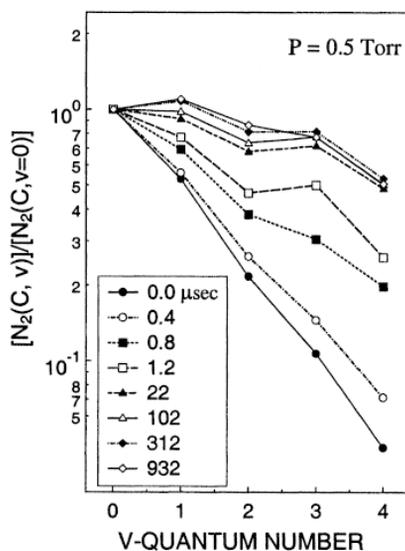
Fig. 1 Time evolution in the post-discharge of $N_2(C^3\Pi_u, v)$ relative distributions: transition from electron impact to excitation by collision processes involving the $N_2(A)$ metastable state.

$N_2(C^3\Pi_u, v)$ in a pulsed N_2 post-discharge. The variation of the distribution shape results from the combined relaxation of the electrons and $N_2(A^3\Sigma_u^+, v)$, both contributing to C-state excitation [12].

Generally, the relaxation of the excited species in post-discharge gives insight to a complementary view of the microscopic kinetics of the discharge. Furthermore, in pulsed discharges the afterglow wall processes of long-lived species can produce memory effects on the discharge regime [40]. On the other hand, metastables can be reformed in post-discharge, creating a significant new ionization, as in the case of the N_2 pink afterglow [33,41].

VIBRATIONAL ENERGY TRANSFERS

The high vibrational excitation of diatomic molecules is the result of the nonresonant and near-resonant vibration–vibration energy transfer (V–V) up-pumping processes, initiated by the electron–vibration excitation (e–V) processes. Vibrational-deactivation (V-T), vibrational-electronic (V-E) processes, and chemical reactions loss processes lead to a Treanor distribution with a plateau and a deactivated tail. These energy transfers have been largely discussed [1,2]. Here we emphasize the collision-induced vibration-to-electronic energy transfers that start when a high vibrational excitation is reached. CO and NO molecules are favorable cases.

Vibrational–electronic energy transfer in CO(X) and NO(X)

The vibrational up-pumping of CO is very effective either when pumped by electrons [19] or by inter-species (V–V') collision as in the case of N_2–CO experiments. The CO vibrational relaxation in a N_2 post-discharge [10] was characterized by three steps: initial N_2–CO (V–V') transfer, CO–CO V–V up-pumping with a long plateau formation (in [10] up to level v = 30) and V–T relaxation by CO_2 product. The modeling of N_2 kinetics in the plasma region, of N_2–CO in the afterglow, and of the CO_2 formation by the associative vibrational mechanism $CO(w) + CO(w) \rightarrow CO_2 + C$ from levels $v \geq 12$, gives account of this view. Similar results were obtained in experiments of CO optical pumping by a cw CO infrared laser [42]. The extremely high vibrational up-pumping reached in these experiments produces

also V–E energy transfer in CO. Despite the weak V–E excitation of $CO(a^3\Pi)$ metastable [19], the V–E excitation of $CO(A^1\Pi)$ state with the appearance of the CO IV-positive system emission is observable. In recent experiments by Rich's group [45–47] this energy transfer was seen to be mediated by low-energy electrons collision with plateau v-levels. This environment can in fact contain a density of electrons comparable to that of a glow discharge (10^{11} cm^{-3}), produced by associative ionization of vibrationally excited molecules. The electrons are then heated by vibrational super-elastic collisions, to a temperature close to 0.5 eV. Moreover, the direct $CO(X, v = 40) + CO \rightarrow CO(A^1\Pi, v' = 0) + CO$ process is not favored by FC factors.

An electron mediated V–E excitation of NO γ and β band emissions is also invoked for NO optically pumped by a CO laser, although only the vibrational excitation of 15 levels was detectable [42 and refs. therein]. A high NO vibrational excitation (up to v = 22) much closer to the electronic $NO(A^2\Sigma_u^+)$ threshold was measured in He–NO discharges [20]. Although the electron impact excitation of NO–γ bands is small compared to other collision mechanisms (see next section), NO–γ band excitation by electron mediated V–E could be significant in presence of a large vibrational excitation. The similarity of the NO distributions in discharge and in optical pumped systems is shown in Fig. 2, where it is also shown how the distribution created by the reaction of $N(^2P, {}^2D)$ with O is different [43]. The modeling of NO vibrational kinetics is still open due to the lack of a reliable data set for V–V and V–T rate coefficients, although state-selected experiments by a pump-probe laser technique have been carried out [48].

V–E transfers have been also considered in the study of the N_2 pink afterglow. This old intriguing issue has been focused by new experiments and kinetic modeling on the re-formation of $N_2(A^3\Sigma_u^+)$ and $N_2(a'^1\Sigma_u^-)$ metastables in post-discharge by two mechanisms based on collisions of $N_2(X, v)$ with $N(^4S)$ [41] or $N(^2P)$ [33] from different v-levels. The evidence of these energy transfers based on the N_2 vibrational relaxation in the post-discharge is however still incomplete.
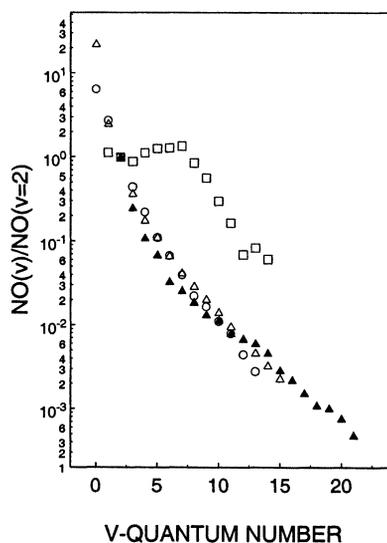
Fig. 2 Measured NO vibrational distributions: (□) nascent from N* + O_2 reaction [43]; (Δ) optical pumping [42]; (○) DC discharge [44]; (▲) RF discharge [20].

ELECTRONIC ENERGY TRANSFERS

The collision-induced electronic transitions are based on spectroscopic perturbations, electrostatic mixing, and spin-orbit mixing [7]. Electronic states with the same multiplicity can be coupled by electro-

static interactions induced by the perturber, while transition between states with different multiplicity can be coupled by the weaker spin-orbit interaction.

He(2^3S) quenching by N_2 and O_2 is well studied in He–N_2 or O_2 pulsed post-discharges. The decay of He metastable monitored by LIF was seen to be well correlated to that of $N_2^+(B\ ^2\Sigma_u^+, w)$ and $O_2^+(B\ ^2\Pi_u^+)$ [49] through the Penning ionization mechanism. The collision-induced state-to-state electronic transitions between the N_2 triplet ($A^3\Sigma_u^+$, $W\ ^3\Delta$, $B'^3\Sigma^-$, $B^3\Pi_g$, $C\ ^3\Pi_u$) states, that produce the excitation of the emitting states $B^3\Pi_g$ and $C\ ^3\Pi_u$, have been largely investigated both in pulsed discharges [12,16,50–52], and in flowing afterglows [33,53–55]. Reactive and nonreactive electronic transfers and collision electronic quenching are important in N_2–O_2 plasmas [31,43,56]. Here we highlight some energy transfers involving $N_2(A^3\Sigma_u^+, v)$ in N_2, N_2–NO, and N_2–H_2O systems [15,57].

$N_2(A^3\Sigma_u, v)$ energy transfer to $N_2(B^3\Pi_u, v)$ and $N_2(C^3\Pi_g, v)$

The collision transfer of $N_2(A^3\Sigma_u^+, w)$ to $N_2(X^1\Sigma_g, v)$ producing $N_2(B\ ^3\Pi_g, v' = 1–12)$ excitation has been well recognized in species-selected afterglow experiments, and the overall rate coefficient was measured in [54]. The details of $N_2(A) + N_2(X) \rightarrow N_2(B) + N_2(X)$ mechanism in N_2 have been pointed out by experiments [58] carried out under single collision condition, employing beam/target arrangements and using N_2 isotopic labeling for the projectile and the target. The process occurs via both intramolecular and intermolecular energy transfer, and $N_2(A)$ or $N_2(X)$ is excited to $N_2(B)$, respectively. The two mechanisms have almost equal importance. The intramolecular energy transfer is confirmed as a quasi-resonance process and populates predominately the high v-levels of B state with close resonance, while the intermolecular one populates predominately the low vibrational levels. The state-to-state cross-sections of the undistinguished (intra-inter) molecular process do not scale according to an FCF energy gap law [4].

Working in a pulsed discharge and modeling the time evolution of $N_2(B, v)$ distributions one recognizes that in early afterglow $N_2(B, v)$ is formed by electron impact from $N_2(X, v)$ manifold as well as from $N_2(A, v)$ [16]. In the late afterglow instead, it is well known that $N_2(B)$ is produced by $N(^4S)$ atoms recombination [59]. The distribution shape changes significantly according to the predominance of the excitation mechanisms. Figure 3 gives an overview of the differences and of the confidence of
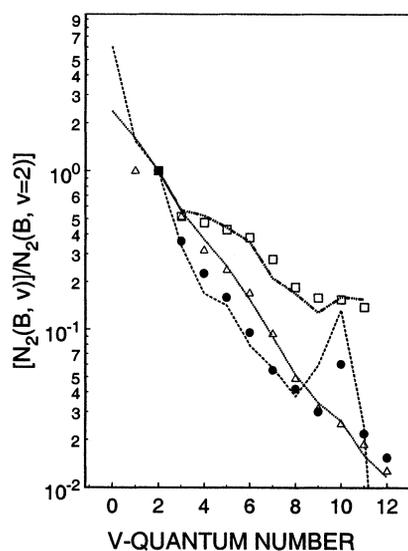
Fig. 3 $N_2(B^3\Pi u, v)$ relative distributions. Experiment and model simulations (see text).

the model simulations. The distribution (□) [53] shows a pure $X + A \rightarrow B + X$ (associative) excitation; distributions (●) and (△) are formed by mixed associative, electron impact from X and A states and pooling $A + A \rightarrow B + X$ processes. This latter process, whose state-to-state rate coefficients were measured by Piper [60], is marked by the overpopulation of level $v = 10$, and is more evident in the distribution (●). The associative $X + A$ process simulation was based on intermolecular process and vibrational state-to-state rate coefficient scaled according to an FCF energy gap law [16,61].

Similarly, the FCF energy gap scaling law was applied to generate state-to-state rate coefficients for the energy transfer excitation of $N_2(C^3\Pi_u, v)$ states by pooling between two $N_2(A^3\Sigma_u^+, w)$ molecules. The state-to-state rate coefficients were measured for $v = 0$ and 1 vibrational levels of A state [55]. Figure 4 shows the C vibrational distribution calculated by this partial set of rate coefficients for a $N_2(A)$ distribution at 2500 K temperature [4]. It is characterized by a significant population inversion in the level $v = 1$, while in that generated by FCFEG scaling law at 400 K gas temperature (1) the maximum is shifted at higher v-levels. The figure also shows the calculated distribution (2) for electron impact process from $N_2(A^3\Sigma_u^+, v)$. The experimental distribution agrees with a mixed excitation by electron from $N_2(A^3\Sigma_u^+, w)$ and pooling (curves 3 and 5). Both pooling rate coefficient data sets give reasonable results. A still open question, finally, concerns the determination of the quenching rates of $N_2(C, v)$ vibrational states [62,63].
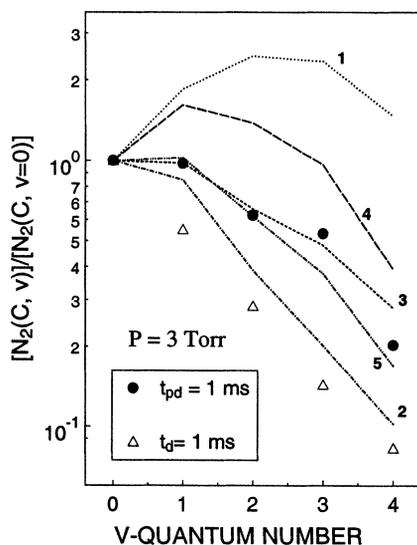
Fig. 4 $N_2(C^3\Pi_u, v)$ relative distributions. Discharge (△) and post-discharge (●) experiments, and model simulations (see text).

$N_2(A^3\Sigma_u^+)$ energy transfer to $NO(A^2\Sigma_u^+)$ and $OH(A^2\Sigma_u^+)$

The energy transfers of $N_2(A^3\Sigma_u^+)$ to NO and OH are interesting cases in pulsed discharges. They show the different features of the excited product depending on whether $N_2(A^3\Sigma_u^+)$ or electrons predominate in the excitation of $NO(A^2\Sigma_u)$ and $OH(A^2\Sigma_u)$. In N_2–NO discharge and post-discharge the electron excitation of NO–γ bands is generally a minor process [15]. The electron mechanism, as can be seen in Ar–NO pulsed discharges, is characterized by a sharp rise and drop of the intensity accompanied by a low rotational excitation of NO(A) state (Fig. 5). On the contrary, the $N_2(A)$ collision transfer leads to a slow rise and decay. The rotational distribution of NO(A, $v = 0$) is non-Boltzmann with a "temperature" of about 1425 K for $J > 20$ and about 900 K for lower J values (Fig. 5). The situation in N_2–O_2 pulsed post-

discharges in which NO is produced by reaction is similar. A similar situation occurs in N_2–H_2O plasma. Whatever is the mechanism forming the OH radical its excitation to the A state takes place by collision energy transfer from $N_2(A)$ [57]. Working in pulsed discharge under weak collision regime the measured quasi-nascent rotational distribution of OH(A) reveals three energy inputs on the rotational level packet close to K = 20, 15, 8, correlated to a quenching transition of $N_2(A)$ toward $N_2(X, v = 5, 6, 7)$, respectively. At higher pressure these details are relaxed by RET collision in OH(A), as shown in Fig. 6.
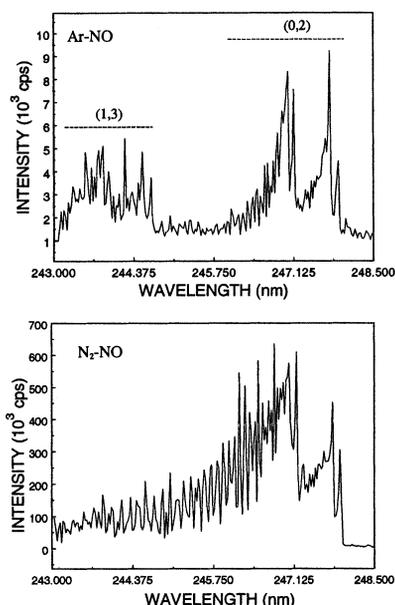
Fig. 5 NO–γ (0,2) band in pulsed discharges with Ar (electron impact excitation) and N_2 [transfer from $N_2(A)$].
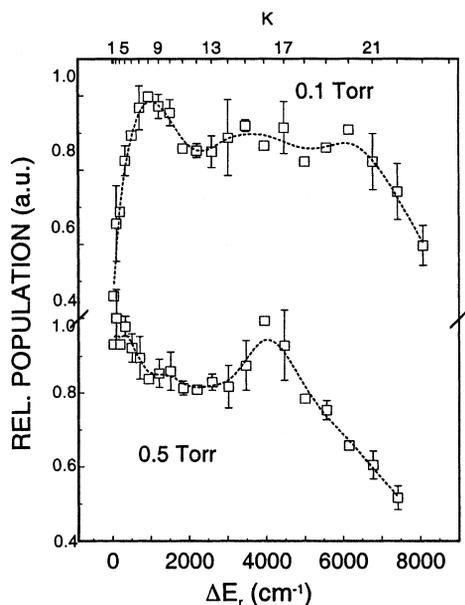
Fig. 6 OH(A, v = 0, K) rotational relative population at 0.1 and 0.5 Torr: effect of RET collisions on the nascent distribution.

CONCLUSIONS

Among the gas phase processes, (V–V') exchanges have been largely considered in the literature of discharge physics, and several calculations have been reported in literature for diatomic molecules and binary mixtures. On the contrary, for the vibrational-to-electronic (V–E) and the electronic-to-electronic (E–E) energy transfers there is a difficulty to calculate rigorously the roto-vibrational state-to-state rate coefficients. Although now the use of molecular beam experiments and laser-selective preparation of initial states are much developed, there is still a lack of data for many molecular systems. Therefore, approximate state-to-state rate coefficients calculated by Franck–Condon Factor energy-gap scaling laws can give account of some structure observed in the measured vibrational distributions.

ACKNOWLEDGMENTS

REFERENCES

1. *"Non-equilibrium Vibrational Kinetics"*, M. Capitelli (Ed.), Topics in Currents Physics, Vol. 39, Springer-Verlag, New York (1986).
2. M. Capitelli, C. M. Ferreira, B. F. Gordiets, A. I. Osipov. *Plasma Kinetics in Atmospheric Gases*, Springer-Verlag, New York (2000).
3. D. H. Katayama and A. V. Dentamaro. *J. Chem. Phys*. **97**, 2820 (1992).
4. R. B. Bachman, X. Li, Ch. Ottinger, A. F. Vilesov, V. Wulfmeyer. *J. Chem. Phys*. **98**, 8606 (1993).
5. V. Aquilanti, R. Candori, F. Pirani, Ch. Ottinger. *Chem. Phys*. **187**, 171 (1994).
6. P. Casavecchia. *Rep. Prog. Phy.* **63**, 355 (2000).
7. P. J. Dagdigian. *Annu. Rev. Phys. Chem*. **48**, 95 (1997).
8. D. W. Setser. *"Quenching reactions of electronically excited atoms"*. APP Spring meeting *"Diagnostics of Non-Equilibrium High Pressure Plasmas"*, B. Honnef and G. Ecker (Eds.), Ruhr-University Bochum (2001).
9. S. De Benedictis. (Guest Ed.), *"Special issue on metastables and long-lived species in ionized gases"*. *J. Phys. D: Appl. Phys*. **34**, (2001).
10. S. De Benedictis, M. Capitelli, F. Cramarossa, C. Gorse. *Chem. Phys*. **111**, 361 (1987).
11. C. Gorse, M. Cacciatore, M. Capitelli, S. De Benedictis, G. Dilecce. *Chem. Phys*. **119**, 63 (1988).
12. S. De Benedictis and G. Dilecce. *Chem. Phys*. **192**, 149 (1995).
13. S. De Benedictis and G. Dilecce. *Plasma Source Sci. Technol*. **4**, 212 (1995).
14. S. De Benedictis and G. Dilecce. *J. Chem. Phys*. **107**, 6219 (1997).
15. S. De Benedictis, G. Dilecce, M. Simek. *J. Phys. D: Appl. Phys*. **30**, 2887 (1997).
16. S. De Benedictis, G. Dilecce, M. Simek. *J. Chem. Phys*. **110**, 2947 (1999).
17. D. W. Setser. *Reactive Intermediates in the Gas Phase*, Academic Press, New York (1979).
18. J. L. Delcroix, C. M. Ferreira, A. Ricard. In *Principles of Laser Plasmas,* G. Bekefi (Ed.), p. 159, Wiley, New York (1976).
19. R. Farrenq, C. Rossetti, G. Guelashivili, W. Urban. *Chem. Phys*. **92**, 589 (1985).
20. S. De Benedictis, G. Dilecce. Procs. ISPC-12 Minneapolis, J. V. Heberlein, D. W. Ernie, J. T. Roberts (Eds.), p. 403 (1995).
21. I. Adamovich, S. Saupe, M. J. Grassi, O. Schulz, S. Macheret, J. W. Rich. *Chem. Phys.* **173**, 491 (1993).
22. B. Massabieaux, G. Gousset, M. Lefebvre, M. Pealat. *J. de Physique* **48**, 1939 (1987).
23. P. Macko, G. Cunge, N. Sadeghi. *J. Phys. D: Appl. Phys*. **34**, 1807 (2001).

24. T. Mosbach and H. F Dobele. Procs. IV-Workshop *"Frontiers of Low Temperature Plasma Diagnostics"*, Rolduc (Netherland), W. W. Stoffels (Ed.), pp. 1–11 (2001).
25. Yu B. Golubovsky, H. Lange, I. A. Porokhova, D. Uhrlandt. *J. Phys. D: Appl. Phys*. **34**, 1840 (2001).
26. M. W. Millard, P. P. Yaney, B. N. Ganguly, C. A. DeJoseph, Jr. *Plasma Source Sci. Technol*. **7**, 389 (1998).
27. J. M. Pouvesle, A. Khacef, J. Stevefelt, H. Jani, V. T. Gylys, C. B. Collins. *J. Chem. Phys*. **88**, 3061 (1988).
28. M. J. Frost, S. Himmelmann, D. D. Palmer. *J. Phys. B: At. Mol. Opt. Phys*. **34**, 1569 (2001).
29. U. Kogelshatz, B. Elliason, W. Egli. *Pure Appl. Chem.* **71**, 1919 (1999).
30. G. J. M. Hagelaar, G. M. W. Kroesen, U. van Slooten, H. Screuders. *J. Appl. Phys*. **88**, 2252 (2000).
31. J. M. Thomas and F. Kaufman. *J. Phys. Chem.* **100**, 8901 (1996).
32. B. Krames, T. Glenewinkel-Meyer, J. Meichsner. *J. Phys. D: Appl. Phys*. **34**, 1789 (2001).
33. N. Sadeghi, C. Foissac, P. Supiot. *J. Phys. D: Appl. Phys*. **34**, 1779 (2001).
34. S. F. Adams and T. A. Miller. *Chem. Phys. Lett*. **295**, 305 (1998).
35. G. Dilecce and S. De Benedictis. *Plasma Source Sci. Technol.* **8**, 2666 (1998).
36. V. Guerra, P. A. Sa, J. Loureiro. *Phys. Rev. E*. **63**, 0464004-1 (2001).
37. G. Colonna and M. Capitelli. *J. Phys. D: Appl. Phys*. **34**, 1812 (2001).
38. A. B. Blagoev, Yu M. Kagan, N. B. Kolokolov, R. I. Lyagushenko. *Sov. Phys. - Tech. Phys.* **19**, 211, 215 (1974)
39. N. A. Gorbunov, N. A. Khromov, N. B. Kolokolov, A. A. Kudriavtsev, R. R. Arslanbekov, A. J. Lediankine. Proc ESCAMPIG 90, Orleans, France, Europhysics Conference Abstracts, Vol. 14 E, B. Dubreuil (Ed.), p. 159 (1990).
40. Z. Li Petrovic, V. Li Markovic, M. M. Pejovic, S. R. Gocic. *J. Phys. D*: *Appl. Phys*. **34**, 1756 (2001).
41. J. Loureiro, P. A. Sa, V. Guerra. *J. Phys. D: Appl. Phys*. **34**, 1769 (2001).
42. S. Soupe, I. Adamovich, M. Grassi, J. W. Rich, R. C. Bergman. *Chem. Phys*. **174**, 219 (1993).
43. W. T. Rawlins, M. E. Fraser, S. M. Miller. *J. Phys. Chem.* **93**, 1097 (1989).
44. R. C. Bergman, M. J. Williams, J. W. Rich. *Chem. Phys*. **66**, 357 (1982).
45. W. Lee, I. V. Adamovich, W. R. Lampert. *J. Chem. Phys*. **114**, 1178 (2001).
46. E. Plonjes, P. Palm, J. W. Rich, I. Adamovich. AIAA 2001-3008, *32nd AIAA Plasmadynamics and Laser Conference*, Anaheim, CA (2001).
47. I. V. Adamovich and J. V. Rich. *J. Phys. D: Appl. Phys*. **30**, 1741 (1997).
48. X. Yang, E. H. Kim, A. M. Wodtke. *J. Chem. Phys*. **96,** 5111 (1992).
49. S. De Benedictis and G. Dilecce. *J. Phys. D: Appl. Phys*. **28**, 2067 (1995).
50. J. S. Morril and W. Benesh *J. Geophys. Res*. **95**, 7711 (1990); *J. Chem. Phys*. **101**, 6529 (1994).
51. E. Agustyniak and J. Borysov. *J. Phys. D: Appl. Phys*. **27**, 652 (1994); **28**, 55 (1995).
52. G. Cartry, L. Magne, G. Cernogora. *J. Phys. D: Appl. Phys*. **32**, 1894 (1999).
53. P. Supiot, D. Blois, S. De Benedictis, G. Dilecce, M. Barj, A. Chapput, O. Dessaux, P. Goudmond *J. Phys. D: Appl. Phys*. **32**, 1887 (1999).
54. L. G. Piper. *J. Chem. Phys*. **91**, 864 (1989).
55. L. G. Piper. *J. Chem. Phys*. **88**, 231 (1988).
56. V. Guerra, P. A. Sà, J. Loureiro. *J. Phys. D: Appl. Phys*. **34**, 1745 (2001).
57. G. Dilecce, M. Simek, S. De Benedictis. *J. Phys. D: Appl. Phys*. **34**, 1799 (2001).
58. Ch. Ottinger, A. F. Vilesov, D. D. Xu. *J. Chem. Phys*. **102**, 1673 (1995) and refs therein.
59. A. Ricard, J. Tetreault, J. Hubert. *J. Phys. B: At. Mol. Opt. Phys*. **24**, 1115 (1991).
60. L. G. Piper. *J. Chem. Phys*. **88**, 6911 (1988).
61. D. H. Katayama, T. A. Miller, V. E. Bondybey. *J. Chem. Phys*. **71**, 1662 (1979).

62. E. Gat, N. Gerardi, S. Lemoing, F. Massines, A. Ricard. *Chem. Phys. Lett*. **306**, 263 (1999).
63. S. V. Pancheshnyi, S. M. Starikovskaia, A. Yu. Starikovskii. *Chem. Phys*. **262**, 340 (2000).